Proceedings of the 4th International Congress APMAS2014, April 24-27, 2014, Fethiye, Turkey

Evaluation of Li-Air Batteries With EC-DEC Based Nanocomposite Electrolytes

A. Akbulut[a,*], M. O. Guler[b], T. Cetinkaya[b], M. Uysal[b], H. Akbulut[b]

[a]Sakarya University, Dept. of Environmental Engineering, Esentepe Campus, 54187, Sakarya, Turkey

[b]Sakarya University, Metallurgy and Materials Engineering, Esentepe Campus 54187 Sakarya, Turkey

Electrolytes based on organic carbonate solvents of ethylene carbonate (EC) and diethyl carbonate (DEC) were prepared by using $LiPF_6$ as the Li-source. Nano sized Al_2O_3 (50 nm) was used as a reinforcing component in order to control corrosion and Li_2CO_3 formation. Corrosion of the Li foil anode and electrochemical tests were performed by using EC/DEC/$LiPF_6$ and nanocomposite EC/DEC/$LiPF_6$/5wt.% Al_2O_3 electrolytes. Electrochemical tests were performed in the swagelok cells by using Li foil anode and carbon air cathode electrodes. Structural tests were carried out by using scanning electron microscopy (SEM), x-ray diffraction (XRD) and Raman spectroscopy. Results revealed that incorporation of nano Al_2O_3 leads to a decrease of corrosion rate of Li anode and a small decrease in the capacity of the air cells.

DOI: 10.12693/APhysPolA.127.1023

PACS: 82.45.Gj, 88.80.ff, 82.45.Xy

1. Introduction

The Li-air battery has the potential to revolutionize energy storage for hybrid and electric vehicles. The high theoretical energy density is associated with Li_2O_2 formation upon charging and discharge processes within a non-aqueous electrolyte [1]. Recent experimental and theoretical studies have shown that commonly used organic carbonates (e.g. propylene carbonate, ethylene carbonate, and dimethyl carbonate) in Li-ion batteries are not stable against oxygen reduction reaction, during discharging processes. In addition, Li_2O_2 and Li_2O are not the major components of the insoluble discharge products. Instead, the products are mainly made of Li_2CO_3 and others, resulting from the decomposition of carbonate electrolytes. Li_2CO_3 is not electrochemically reversible in the aprotic lithium-air battery systems, which will limit their chargeability, cycle life, and stability in lithium-air batteries. The addition of inorganic fillers such as silica (SiO_2), or aluminum oxide (Al_2O_3) or titania (TiO_2) nanoparticles into the electrolyte results in the enhancement of physical strength as well as the increase in the absorption level of electrolyte solution [2]. Moreover inorganic fillers also act as solid plasticizers, hindering the reorganization of polymer chains and can interact with polar groups by Lewis acid-base reaction. As a result, the properties such as ionic conductivity, lithium ions transference number and activation energy for ionic transportation are improved [3]. In this paper, we report the effects of addition of large quantities of nano Al_2O_3 on hydrophobic ionic liquid electrolytes. Nano Al_2O_3 particles were added into the EC/DEC/$LiPF_6$ in order to obtain stable electrolyte systems for Li-Air energy storage devices. The corrosion behavior of the metallic lithium cathode and the specific capacity of the battery were also studied.

2. Experiment details

The phase constituents of the samples were determined by powder XRD with a Rigaku D/MAX 2000 X-ray generator and diffractometer with CuK_α radiation. The diffraction patterns were collected in step scan mode and recorded in 1° (2θ) steps, at 1 min per step, in the range $10° < 2\theta < 80°$. SEM (Jeol 6060LV) was used to investigate the microstructure of samples. The Raman spectroscopy was performed by Kaiser Optical RAMAN-RXN1 microprobe, using a 785 nm Invictus laser light source with excitation power of 50 mW. The Raman shifts were collected in a range of 300–3000 cm^{-1}. In order to evaluate the corrosion performance of electrolytes, linear polarization studies were carried out using Gamry Instruments Reference 3000. Stainless steel plate was used as the cathode, while metallic lithium was used as the reference electrode. The electrolyte used was 1 M $LiPF_6$ dissolved in EC:DEC (1:1 by vol.) solution.

In order to evaluate the electrochemical performance of the as-produced electrolytes, ECC-Air cells were assembled in argon filled glove-box. Metallic lithium foil was used as anode electrode, while Sigracet 24BC gas diffusion layer (GDL) was used as the counter electrode. A separator, based on glass fibers, was also used in order to prevent a shortcut between the electrodes. The cells were cyclically tested on a MTI Model BST8-MA electrochemical analyzer, using current density of 0.1 mA/cm^2, over a voltage range of 2.15–4.25 V. The effect of nano alumina addition on the electrochemical properties was investigated. Two different electrolytes were prepared as EC/DEC/$LiPF_6$ and nanocomposite electrode of EC/DEC/$LiPF_6$/5 wt.% Al_2O_3 (50 nm). Electrochemical impedance spectroscopy (EIS) measurements were also conducted before and after the galvano-

*corresponding author; e-mail: aakbulut@sakarya.edu.tr

static tests in order to evaluate the effect of inorganic additives on the battery performance.

3. Results and discussion

In order to evaluate the effect of the alumina addition on the chemical and morphological variations in the cathode electrodes, SEM and XRD analyses were performed over the surfaces of GDL air breathing cathodes. The surfaces of the GDLs were examined after the battery tests and the results are presented in Fig. 1. As can be seen from Fig. 1a, after discharge, the extensive accumulation of solid Li_2CO_3 on the porous cathode can block the oxygen diffusion at the electrode/air interface, leading to the failure of further discharge processes for the EC/DEC/$LiPF_6$ electrolyte. Introduction of 5 wt.% of nano Al_2O_3 particles into the electrolytes resulted in reduction of the amount of the air blocking phases. The surfaces of the GDL air cathode, reinforced with the nanocomposite electrolyte, have shown porosities and the fibrous phases belonging to the glass fibers coming from the glass separator.

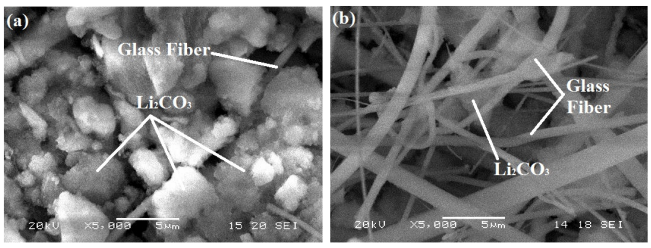

Fig. 1. SEM images of the GDL cathode surfaces after electrochemical test of the electrolytes: (a) EC/DEC/$LiPF_6$ and (b) EC/DEC/$LiPF_6$/5 wt.% Al_2O_3.

The corrosion tests were performed for two electrolyte samples. The anodic and cathodic corrosion curves are shown in Fig. 2a. As it is demonstrated, introduction of 5 wt.% of nano Al_2O_3 particles resulted in an increase of the passivation of the anodic reaction, which is a beneficial effect for the protection of the Li anode from corrosion in the Li-air cells. The corrosion test results are summarized in Table. The corrosion potentials, corrosion current densities and anodic/cathodic Tafel slopes (β_a and β_c) were calculated. Based on the approximate linear polarization at the corrosion potential (E_{corr}), corrosion current (I_{corr}) and polarization resistance (R_p) values were determined using equation

$$I_{\mathrm{corr}} = \frac{1}{2.303 R_p}\left(\frac{\beta_a \beta_c}{\beta_a + \beta_c}\right), \qquad (1)$$

where β_a and β_c respectively referred to anodic and cathodic Tafel slope in Volts/decade or mV/decade of current density, I_{corr} is the corrosion current density in mA/cm^2, R_p is the corrosion resistance in $\Omega\,$cm^2.

Figure 2b shows the XRD patterns for the GDL surfaces after cycling of the EC/DEC/$LiPF_6$ and EC/DEC/$LiPF_6$/5 wt.% Al_2O_3. As can be concluded

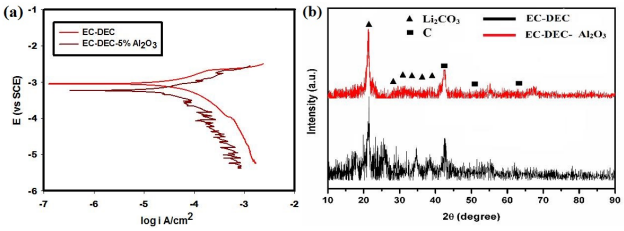

Fig. 2. (a) Anodic and cathodic corrosion curves and (b) XRD patterns for the GDL surfaces after cycling with the EC/DEC/$LiPF_6$ and EC/DEC/$LiPF_6$/5 wt.% Al_2O_3.

TABLE Corrosion results for EC/DEC/$LiPF_6$ and EC/DEC/$LiPF_6$/5 wt.% Al_2O_3 electrolytes.

Electrolyte	E_{corr} [mV](vs. Eoc)	I_{corr} [mA/cm^2]	R_p [$\Omega\,$cm^2]
$LiPF_6$-EC-DEC	-315.1	0.04211	1.4
$LiPF_6$-EC-DEC-Al_2O_3	-308.8	0.03869	1.6

from the XRD results, introduction of 5 wt.% of Al_2O_3 into the electrolyte has significantly reduced the intensity of Li_2CO_3 phases over the GDL cathode surface. For further characterization, the Raman spectra of the GDL surfaces after electrochemical tests were also studied and results are shown in Fig. 3.

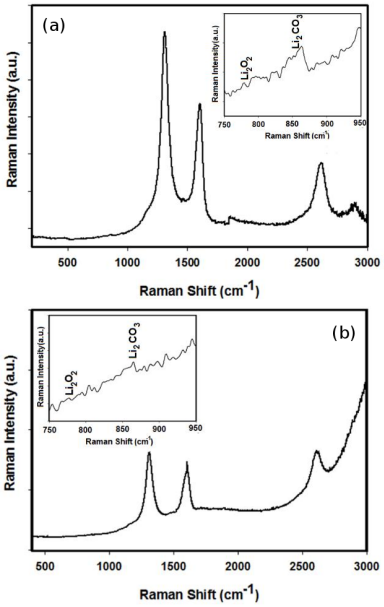

Fig. 3. Raman spectra of GDL air cathode for (a) EC/DEC/$LiPF_6$ and (b)EC/DEC/$LiPF_6$/5 wt.% Al_2O_3 after electrochemical cyclic test. The insets show magnification of a region of Raman spectrum with small intensity.

Figure 3a shows that the GDL surface after tests with EC/DEC/$LiPF_6$ presents a very strong peak at 1310 cm^{-1}, 1580 cm^{-1} and 2651 cm^{-1}, which could be attributed to the D, G and G^1 bands of the carbon, respectively. In the case of nanocomposite electrolyte the D band intensity decreases. On the magnified Raman

spectrum between 750 and 950 cm^{-1} (insets in Fig. 3), it can be seen that the Li_2CO_3 formation is more dominant in the EC/DEC/$LiPF_6$ electrolyte. Li_2O_2 peak is also observed in both electrolytes. However, the intensity of Li_2O_2 peak is decreased with the addition of 5 wt.% of Al_2O_3, which could be attributed to better reduction of Li_2O_2 [4].

The charge-discharge potential profiles of Li-air cells at a current rate of 0.1 mA/cm^2 between 2.15 and 4.25 V vs. Li^+/Li are shown in Fig. 4. An open circuit potential (OCV) value of 3.015 V vs. Li^+/Li is recorded for the tested cells. The open circuit voltage of the sample is compatible with the literature data obtained for a Li-air cell with carbon cathodes (2.9–3.1 V vs. Li^+/Li) [5]. The discharge capacities presented here are the actual capacities without processing with the carbon weight. Introduction of Al_2O_3 into the EC/DEC/$LiPF_6$ electrolyte resulted in a significant increase of the discharge capacity. It is suggested that the fast piling up of solid Li_2O_2 together with nano Al_2O_3 particles onto the porous cathode can block the oxygen diffusion at the electrode/air interface, leading to a failure at the end of discharge processes.

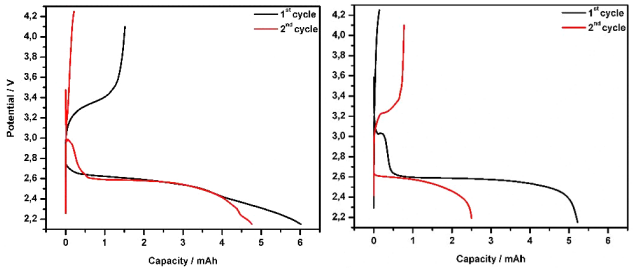

Fig. 4. Voltage-capacity curves for the Li-air cell with (a) EC/DEC/$LiPF_6$ and (b) EC/DEC/$LiPF_6$/5 wt.% Al_2O_3 as electrolytes, cycled at 0.1 mA/cm^2 between 2.15 V and 4.25 V.

The Nyquist plots of Li-air cells are presented in Fig. 5. It is well known that the diameter of the semicircle in the high-frequency region (HF) is mainly induced by the intrinsic electronic resistance and contact resistance of the electrode. It can be concluded from the figure with EIS spectra, that the diameter of semi-circles, is increasing due to pulverization of electrodes after each cycle, and this leads to loss of electronic contact between electrolyte and electrodes. In spite of fact that EC/DEC/$LiPF_6$ electrolyte leads to production of higher electronic contact resistance, analysis after the discharge process has revealed, that the higher resistance is caused by the blocking of the air cathode by Li_2O_2, Li_2CO_3 and nano Al_2O_3 particles on the air side, after the electrochemical cycling test [6].

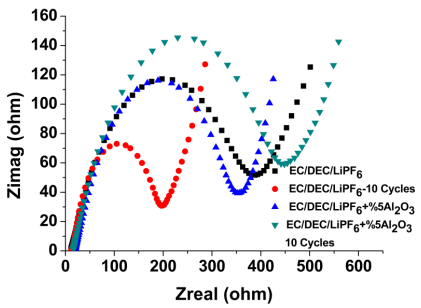

Fig. 5. Nyquist plots of Li-air cells for two different electrolytes before and after cycles.

4. Conclusions

Introduction of nano sized (50 nm) 5 wt.% Al_2O_3 particles into the EC/DEC/$LiPF_6$ electrolyte resulted in the increasing corrosion resistance of the Li foil anodes. Incorporation of Al_2O_3 nano particles into the electrolyte results in formation of smaller amount of Li_2CO_3 and at the same time smaller amount of Li_2O_2. The discharge capacity of the nanocomposite EC/DEC/$LiPF_6$/5 wt.% Al_2O_3 yielded lower values, since the nano particles decreased the reaction and led to blocking of GDL cathode air breathing pores and also resulted in increasing contact resistance of the electrodes, because of insulating nature of the nano ceramic powders. Therefore, it is concluded from this work that introduction of inorganic nano particles is beneficial for preventing anode corrosion but needs to be optimized for better future high performance Li-air cells.

Acknowledgments

This research has received funding from the Seventh Framework Programme FP7/2007–2013 (Project STABLE – Stable high-capacity lithium-Air Batteries with Long cycle life for Electric cars) under grant agreement 314508.

References

[1] P.G. Bruce, S.A. Freunberger, L.J. Hardwick, J.M. Tarascon, *Nature Materials* **11**, 19 (2012).

[2] Z. Li, G. Su, D. Gao, X. Wang, X. Li, *Electrochimica Acta* **49**, 4633 (2004).

[3] P.A.R.D. Jayathilaka, M.A.K.L. Dissanayake, I. Albinsson, B.E. Mellander, *Electrochimica Acta* **47**, 3257 (2002).

[4] J. Wang, Y. Li, X. Sun, *Nano Energy* **2**, 443 (2013).

[5] J. Adams, M. Karulkar, V. Anandan, *J. Power Sources* **239**, 132 (2013).

[6] G.Q. Zhang, J.P. Zheng, R. Liang, C. Zhang, B. Wang, M. Hendrickson, E.J. Plichta, *J. Electrochem. Soc.* **157**, A953 (2010).